POLITECNICO
MILANO 1863

SCUOLA DI INGEGNERIA INDUSTRIALE
E DELL'INFORMAZIONE

Executive Summary of the Thesis

Decentralized Spacecraft Formation Reconfiguration Exploiting a Shape-Based Method for Trajectory Optimization

Laurea Magistrale in Space Engineering - Ingegneria Spaziale

Author: Matteo Brioschi

Advisor: Prof. Mauro Massari

Academic year: 2021-2022

1. Introduction

In the last two decades, the space segment has been characterized by two major trends: the increase in satellites' launch rates and the decrease in the satellites' dimensions. As a consequence, not only the number of satellites orbiting Earth has increased, but also the strategy of distributed systems, in the form of constellations and formation flying missions, is becoming more widespread.
The main objective of this work is to develop a tool for formation reconfiguration for satellites flying in close-range. Two cornerstones have been set: perform trajectory optimization by means of a shape-based method and perform formation reconfiguration by means of a decentralized approach. The reason behind these cornerstones is to increase the autonomy of satellites from ground stations, which will be not only desirable but also mandatory, as their number increases. In particular, shape-based methods allow to obtain a feasible solution with a low computational effort when dealing with satellites capable to perform maneuvers with continuous thrust. A decentralized approach, instead, allows to spread the computational burden among all the satellites of the formation and increases the reliability of the overall mission.

The solution of the trajectory optimization problem by means of a shaped-based method has been tackled by a wide variety of shape functions, the most commons being polynomials [1], exponential sinusoid [2], the Fourier series [3], and the Bézier one [4].
Concerning formation reconfiguration, possible approaches to such problem are: disciplined convex programming, collective control [5], direct approach [6], and a centralized approach by means of a shape-based method [4].
This work is structured as follows: Sec. 2 presents the dynamical model, Sec. 3 deals with the trajectory optimization problem, Sec. 4 shows the testing of the developed model and an analysis on how the results of the optimization process are affected by the order of the Bézier series. Finally, Sec. 5 deals with the formation reconfiguration problem solving it by means of a decentralized approach.

2. Dynamical Models

To describe the dynamics of the involved satellites two different reference frames have been used: the Earth-Centered Inertial (ECI) reference frame and the Local-Vertical-Local-Horizontal (LVHL) reference frame, centered in the leader satellite and moving with it.

The equations of motion for each satellite in the ECI can be expressed as follows:

$$\ddot{\boldsymbol{R}}_{\boldsymbol{I}} = -\frac{\mu}{R_I^3}\boldsymbol{R}_{\boldsymbol{I}} + \boldsymbol{F}_{\boldsymbol{I}}(t) \tag{1}$$

In which $\boldsymbol{R}_{\boldsymbol{I}}$ is the position vector, the subscript $\boldsymbol{I}$ is used to identify the satellite I, μ is the Earth's gravitational constant, and $\boldsymbol{F}_{\boldsymbol{I}}$ is the applied control.

2.1. Hill-Clohessy-Wiltshire Model

In this work, the Hill-Clohessy-Wiltshire (HCW) equations have been used to describe the relative dynamics between the leader and the follower satellites. The HCW model is obtained by means of a linearization of the relative motion between the two satellites. The dynamics of the follower satellite are described in the LVLH reference frame as follows:

$$\begin{aligned} \ddot{x} - 2N\dot{y} - 3N^2 x &= f_x \\ \ddot{y} + 2N\dot{x} &= f_y \\ \ddot{z} + N^2 z &= f_z \end{aligned} \tag{2}$$

In which:

- f_x, f_y, and f_z are the thrust acceleration components of the control.
- $N = \sqrt{\mu/a_L^3}$ is the average orbital angular velocity of the leader satellite and a_L is its semi-major axis.

This model is suitable when the leader satellite is flying on a circular orbit, the propagation time is at most one orbital period, and the satellites are in close formation. Note that this model does not include perturbative effects since their differential effect, between leader and follower satellites, is negligible when the distances between the involved satellites are within tens of meters.

3. Trajectory Optimization

The minimization problem to be solved is the following: minimize the ΔV of a satellite that has to change its configuration with respect to a leader satellite. Such satellite is subjected to two constraints:

- The total thrust acceleration, $f(t)$, must be lower than the maximum available one, f_{max}.
- The distance between the leader and the follower satellites, $d_{LF}(t)$, must be higher than a given threshold value, d_{min}.

The mathematical statement of the optimization problem is the following:

$$\begin{aligned} \min_{x,y,z} \quad & \Delta V = \int_0^T f(t)\,dt \\ s.t. \quad & \begin{cases} (f(t))^2 - f_{max}^2 \leq 0 \\ d_{min}^2 - (d_{LF}(t))^2 \leq 0 \end{cases} \end{aligned} \tag{3}$$

In which T is the maneuvering time.
The total thrust acceleration, $f(t)$, and the distance between leader and follower satellites are computed as follows:

$$f(t) = \sqrt{(f_x(t))^2 + (f_y(t))^2 + (f_z(t))^2} \tag{4}$$

$$d_{LF}(t) = \sqrt{(x(t))^2 + (y(t))^2 + (z(t))^2} \tag{5}$$

In which $f_x(t)$, $f_y(t)$, and $f_z(t)$ are the thrust acceleration components of the follower satellite while $x(t)$, $y(t)$, and $z(t)$ are its position components in the LVLH reference frame.
Note that the nonlinear inequality constraints have been expressed by means of their square values to provide to the optimizer a region of feasible solutions broader than the one provided by the square root of the same expressions.
The optimization problem has twelve boundary conditions in the form of initial and final states of the follower satellite in the LVLH reference frame:

$$\begin{bmatrix} x_0 & y_0 & z_0 & \dot{x}_0 & \dot{y}_0 & \dot{z}_0 \end{bmatrix}$$
$$\begin{bmatrix} x_T & y_T & z_T & \dot{x}_T & \dot{y}_T & \dot{z}_T \end{bmatrix}$$

3.1. Bézier Shape Function

The Bézier series is defined as follows:

$$a(\tau) = \sum_{j=0}^{n} B_j(\tau) P_j = \boldsymbol{B}(\tau)\boldsymbol{P} \tag{6}$$

In which n is an integer that represents the order of the Bézier series, P_j are the geometric coefficients, and $B_j(\tau)$ are the Bernstein polynomials. It is worth highlighting that the Bernstein polynomials form a complete basis over the interval $[0, 1]$ for all polynomials of degree $\leq n$.
The first and second τ derivatives of the Bézier series are the following:

$$a'(\tau) = \sum_{j=0}^{n} B_j'(\tau) P_j = \boldsymbol{B'}(\tau)\boldsymbol{P} \tag{7}$$

$$a''(\tau) = \sum_{j=0}^{n} B_j''(\tau) P_j = \boldsymbol{B''}(\tau)\boldsymbol{P} \tag{8}$$

Note that the geometric coefficients do not depend on τ and remain constant upon derivation.

3.1.1 Components of the Follower Satellite by Means of the Bézier Series

Due to the definition of the Bézier series, it is necessary to define a scaled time that ranges in the interval $[0, 1]$:

$$\tau = t/T \tag{9}$$

In which t is the time variable that ranges between 0 and T.
With this scaling, the velocity and the acceleration components are now expressed as follows:

$$\dot{\boldsymbol{x}}(t)T = \boldsymbol{x'}(\tau) \tag{10}$$
$$\ddot{\boldsymbol{x}}(t)T^2 = \boldsymbol{x''}(\tau) \tag{11}$$

In which the notation $\cdot$ represents the time derivative while the subscript $'$ represents the τ derivative.
It is now possible to express the position, velocity, and acceleration components by means of the Bézier series:

$$\boldsymbol{x}(\tau) = \begin{bmatrix}\boldsymbol{B_x P_x} & \boldsymbol{B_y P_y} & \boldsymbol{B_z P_z}\end{bmatrix} \tag{12}$$
$$\boldsymbol{x'}(\tau) = \begin{bmatrix}\boldsymbol{B'_x P_x} & \boldsymbol{B'_y P_y} & \boldsymbol{B'_z P_z}\end{bmatrix} \tag{13}$$
$$\boldsymbol{x''}(\tau) = \begin{bmatrix}\boldsymbol{B''_x P_x} & \boldsymbol{B''_y P_y} & \boldsymbol{B''_z P_z}\end{bmatrix} \tag{14}$$

Note that the subscripts x, y, and z indicate that each component might have a different order of the Bézier series and that the geometric coefficients are different for each component.
The boundary conditions allow to compute four geometric coefficients for each component; this is possible due to the fact that for the Bernstein polynomials the following is valid:

$$\begin{aligned}
\boldsymbol{B}(0) &= \begin{cases} 1 & j = 0 \\ 0 & j \in [1, n] \end{cases} \\
\boldsymbol{B}(1) &= \begin{cases} 0 & j \in [0, n-1] \\ 1 & j = n \end{cases} \\
\boldsymbol{B'}(0) &= \begin{cases} -n & j = 0 \\ n & j = 1 \\ 0 & j \in [2, n] \end{cases} \\
\boldsymbol{B'}(1) &= \begin{cases} 0 & j \in [0, n-2] \\ -n & j = n-1 \\ n & j = n \end{cases}
\end{aligned} \tag{15}$$

Therefore, for the x component the following is valid:

$$\begin{aligned}
x(0) &= x_0 = P_{0,x} \\
x(1) &= x_T = P_{n_x,x} \\
x'(0) &= \dot{x}_0 T = -n_x P_{0,x} + n_x P_{1,x} \\
x'(1) &= \dot{x}_T T = -n_x P_{n_x-1,x} + n_x P_{n_x,x}
\end{aligned} \tag{16}$$

In which n_x is the order of the Bézier series of the x component. The same can be written for the y and z components.
The set of equations above shows that, for each component, four geometric coefficients can be determined by means of the boundary conditions. Also note that, if $n_x = n_y = n_z = 3$ there will be four unknown geometric coefficients for each component that can be determined by imposing the boundary conditions.

3.2. Optimization Problem by Means of a Shape-Based Method

Concerning the implementation, to ease the optimization process, the involved quantities have been made dimensionless in space and time; the latter is also a requirement of the Bézier series. This process is performed by either multiplying or dividing the involved quantities by the time of flight (or its square value) and by a space scaling. The latter is the maximum, in absolute value, of the position components obtained with a third order Bézier series and the given boundary conditions.
After this process, the overall structure of the problem is still the same as the one presented in Eq. (3). The main differences are that the involved quantities are now in dimensionless form and the optimization variables are different. Indeed, the optimization variables are the unknown geometric coefficients of the three components of the follower satellite. In particular, because the boundary conditions allow to compute the first two and the last two geometric coefficients for each component, there will be a number of optimization variables equal to:

$$n_x + n_y + n_z - 9 \tag{17}$$

Finally, note that the first guess of the geometric coefficients, that are also the optimization variables, is obtained by data fitting of the trajectory obtained from a third order Bézier series.

4. Testing of the Model

The developed optimizer has been tested by comparing the results with data available from literature [4]. The most relevant parameters are the following:

- The minimum distance between the leader and the follower satellite is 1.6 m.
- The maximum thrust acceleration is 6×10^{-3} m/s^2.
- The time of flight is 300 s.
- The order of the Bézier series for each coordinate is $\boldsymbol{n} = [12 \quad 12 \quad 16]$.

Several test cases have been performed, below is reported the result for one of those.

The initial and final positions, in meters, of the follower satellite are, respectively, $(-1.5, -3, -3)$ and $(1, 2, 1.5)$, while the initial and final relative velocities are equal to 0. The ΔV obtained in literature is equal to 0.083 m/s while the one obtained with the developed optimizer is equal to 0.078 m/s. Considering the computation time, the one obtained in literature is equal to 138.848 s while the one obtained with the developed optimizer is equal to 13.204 s. Three remarks:

- All the tests of the developed optimizer were carried out on a i7-4720HQ 2.60 GHz processor, 16.0 GB RAM, with Windows 10 and run on MATLAB R2022b.
- In the developed optimizer the time of flight is not an optimization variable while in literature it is.
- In the developed optimizer only one satellite is considered while in literature three satellites are considered simultaneously; this explains the high difference between the computation times of the two methods.

Figure 1 and Figure 2 show, respectively, the obtained thrust acceleration history and the distance between the leader and the follower satellites as a function of time. It can be noted that the obtained total thrust acceleration tries to resemble a bang-bang solution, which is the optimal one when dealing with the fuel-optimal problem; such solution cannot be obtained by means of the implemented method due to the mathematical description of the shape function. It is also worth noting that the follower satellite tends to get closer to the leader one, up until the safe distance is reached, and then reaches the final boundary condition.

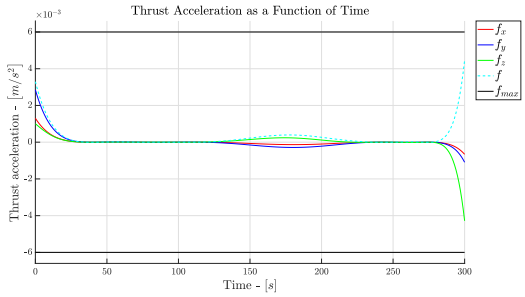

Figure 1: Total Thrust Acceleration and Thrust Acceleration Components as a Function of Time.

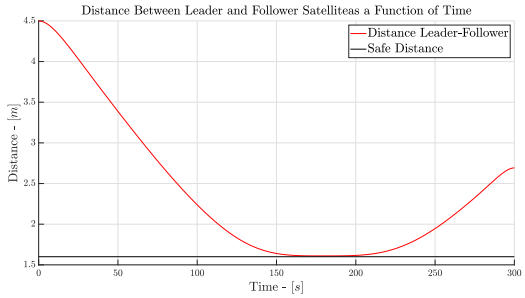

Figure 2: Distance Between the Satellites.

4.1. An Analysis on the Order of the Bézier Series

Figure 3 shows the ΔV as a function of the order of the Bézier series for the case presented in Sec. 4. It can be noted that the ΔV decreases for increasing orders of the Bézier series up to $\boldsymbol{n} = 10$; instead, when the order is $\boldsymbol{n} \geq 12$ the ΔV remains almost constant.

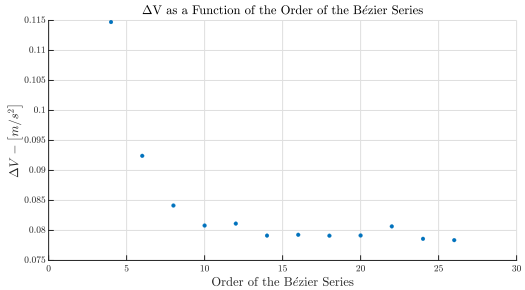

Figure 3: ΔV as a Function of the Bézier Series.

Figure 4 shows the thrust acceleration components and the total thrust acceleration as a function of time, for the case presented in Sec. 4. It is worth noting that for lower orders of the Bézier series, $\boldsymbol{n} \leq 10$, the thrust acceleration profiles are quite simple and resemble a second or third order polynomial; this is expected since Bézier series of lower orders are limited in terms of the possible functions that they can represent

and, therefore, only simple functions can be obtained. For higher orders of the Bézier series, $\boldsymbol{n} \geq 12$, the thrust acceleration profiles remain almost unchanged, since an optimal solution has been reached and a different profile would lead to a higher ΔV.

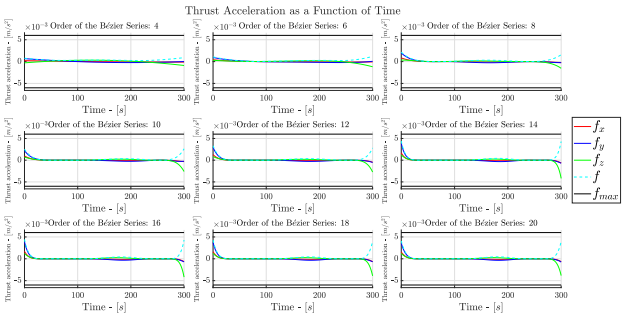

Figure 4: Thrust Acceleration as a Function of Time for Different Orders of the Bézier Series.

5. Formation Reconfiguration

When dealing with circular orbits, once the trajectory of a follower satellite is computed, such result is valid at any point along the orbit. Therefore, collision avoidance between the follower satellites can be enforced by time-shifting the starting maneuvering time of each satellite. The most relevant aspects of the developed algorithm, shown in Figure 5, are the following:

- If reconfiguration is not possible by maneuvering all the satellites at the same time, a genetic algorithm is executed. Such algorithm tries to minimize the starting maneuvering times while enforcing a minimum distance between the satellites.
- In case such algorithm fails, the trajectory of the satellites that get too close to each other is computed again with additional constraints in the form of a minimum distance with respect to the initial and final positions of the involved satellites.
- After computing the new trajectory, the same genetic algorithm is executed again to obtain a feasible reconfiguration.
- The last two points are repeated in a *while* loop, in which the minimum distance mentioned above is progressively increased until a possible reconfiguration is obtained, or the maximum value of the minimum distance is reached; if the latter condition is reached, reconfiguration is not possible.

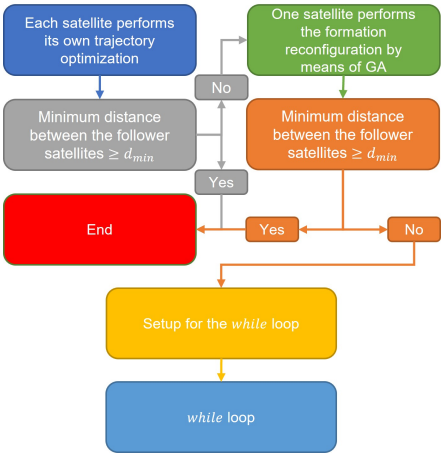

Figure 5: Reconfiguration Algorithm.

5.1. Testing of the Developed Algorithm

The developed algorithm has been tested by comparing the results with data available from literature [4]. The most relevant parameters are the same as the ones presented in Sec. 4.
Three satellites have been considered: their initial positions in meters are respectively $(2, -3, 0)$, $(-1.5, -3, 3)$, and $(-1.5, -3, -3)$; their final positions are respectively $(-2, 2, 0)$, $(1, 2, -1.5)$, and $(1, 2, 1.5)$. The initial and final relative velocities are equal to 0. In Table 1 are reported the results of the reconfiguration and are compared with the data from literature. Note that the computation time is obtained by assuming that the trajectory optimization is simultaneously performed by each satellite. The ΔV is lower than the one obtained in literature and the total time of flight is higher; this is expected due to the idea behind the algorithm. Conversely, the computation time is higher than the one in literature because it was necessary to compute new trajectories.

	Literature	Algorithm
Total ΔV	0.238 m/s	0.234 m/s
Flight Time	299.992 s	525.711 s
Comp. Time	233.338 s	406.101 s

Table 1: Results of Formation Reconfiguration.

Figure 6 shows the distances between all the satellites in two cases: in the top part such distances are obtained in case all the satellites perform the reconfiguration maneuvers simulta-

neously; in the bottom part, instead, after the reconfiguration algorithm. Figure 7 shows the trajectories for all the satellites: the initial trajectories are on the left side and are obtained without the introduction of the additional constraints; on the right side are the final ones, obtained after the execution of the reconfiguration algorithm. It can be noted that the trajectories of satellites 5 and 6 have been changed to make the formation reconfiguration possible.

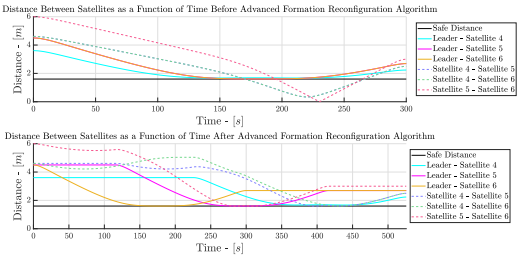

Figure 6: Distance Between Satellites When Maneuvers are Performed Simultaneously (Top) and After Reconfiguration Algorithm (Bottom).

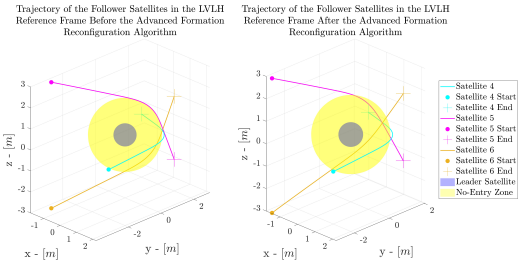

Figure 7: Trajectory of the Satellites Before (Left) and After (Right) the Algorithm.

Three important considerations: the comparison, in terms of ΔV, with the literature is only related to the quality of the reconfiguration but the two results cannot be compared directly because an equal time window would be required. The second consideration relates to the conditions of the satellites before and after the reconfiguration: as shown in Figure 6, the satellites remain fixed in either the initial and/or the final positions depending on the starting maneuvering times. To do so an additional control is necessary; in the considered scenario it is negligible because the initial and final relative velocities are equal to zero. Therefore, the developed tool works well when a zero velocity at the boundaries is assumed and, in case this condition cannot be imposed, not only a poor solution might be obtained, but also errors could arise.

6. Conclusions

Trajectory optimization has been successfully performed by means of a shape-based method exploiting the Bèzier series. The main lesson that has been learned is that, even increasing the order of the Bézier series, the obtained result is limited by the mathematical nature of the shape function.
Considering now formation reconfiguration, this optimization problem has been tackled by means of a decentralized approach; this choice is dictated by the goal of achieving a higher autonomy with respect to ground stations. Concerning the developed algorithm, it has been proved to be working correctly when tested with data from literature. Nonetheless it has some limitations related to the conditions of the satellites.

References

[1] F. T. Johnson, "Approximate finite-thrust trajectory optimization.," *AIAA Journal*, vol. 7, no. 6, pp. 993–997, 1969.

[2] A. E. Petropoulos and J. M. Longuski, "Shape-based algorithm for the automated design of low-thrust, gravity assist trajectories," *Journal of Spacecraft and Rockets*, vol. 41, no. 5, pp. 787–796, 2004.

[3] E. Taheri and O. Abdelkhalik, "Shape based approximation of constrained low-thrust space trajectories using fourier series," *Journal of Spacecraft and Rockets*, vol. 49, no. 3, pp. 535–546, 2012.

[4] Z. Fan, M. Huo, S. Xu, J. Zhao, and N. Qi, "Fast cooperative trajectory optimization for close-range satellite formation using bezier shape-based method," *IEEE Access*, vol. 8, pp. 30918–30927, 2020.

[5] M. Sabatini and G. B. Palmerini, "Collective control of spacecraft swarms for space exploration," *Celestial Mechanics and Dynamical Astronomy*, vol. 105, no. 1–3, p. 229–244, 2009.

[6] R. Armellin, M. Massari, and A. E. Finzi, "Optimal formation flying reconfiguration and station keeping maneuvers using low thrust propulsion," in *Proceedings of the 18th International Symposium on Space Flight Dynamics (ESA SP-548)*, pp. 429–434, 2004.